

Transformation of cyclodextrin glucanotransferase (CGTase) from aqueous suspension to fine solid particles via electrospraying

Suryani Saallah^{a,b}, M. Nazli Naim^{a,*}, Mohd. Noriznan Mokhtar^a, Noor Fitrah Abu Bakar^c, Masao Gen^e, I. Wuled Lenggoro^{d,e}

^a Department of Process and Food Engineering, Faculty of Engineering, Universiti Putra Malaysia, 43400 Serdang, Selangor, Malaysia

^b Biotechnology Research Institute, Universiti Malaysia Sabah, 88400 Kota Kinabalu, Sabah, Malaysia

^c Faculty of Chemical Engineering, Universiti Teknologi MARA, 40450 Shah Alam, Selangor, Malaysia

^d Department of Chemical Engineering, Tokyo University of Agriculture and Technology, 2-24-16 Nakacho, Koganei, Tokyo 184-8588, Japan

^e Graduate School of Bio-Applications and Systems Engineering, Tokyo University of Agriculture and Technology, 2-24-16 Nakacho, Koganei, Tokyo 184-8588, Japan

ARTICLE INFO

Article history:

Received 10 November 2013

Received in revised form 17 June 2014

Accepted 21 June 2014

Available online 7 July 2014

Keywords:

Electrospraying
Droplet fission
Solidified enzyme
Enzyme activity

ABSTRACT

In this study, the potential of electrohydrodynamic atomization or electrospraying to produce nanometer-order CGTase particles from aqueous suspension was demonstrated. CGTase enzyme was prepared in acetate buffer solution (1% v/v), followed by electrospraying in stable Taylor cone-jet mode. The deposits were collected on aluminium foil (collector) at variable distances from the tip of spraying needle, ranging from 10 to 25 cm. The Coulomb fission that occurs during electrospraying process successfully transformed the enzyme to the solid state without any functional group deterioration. The functional group verification was conducted by FTIR analysis. Comparison between the deposit and the as-received enzyme in dry state indicates almost identical spectra. By increasing the distance of the collector from the needle tip, the average particle size of the solidified enzyme was reduced from 200 ± 117 nm to 75 ± 34 nm. The average particle sizes produced from the droplet fission were in agreement with the scaling law models. Enzyme activity analysis showed that the enzyme retained its initial activity after the electrospraying process. The enzyme particles collected at the longest distance (25 cm) demonstrated the highest enzyme activity, which indicates that the activity was controlled by the enzyme particle size.

© 2014 Elsevier Inc. All rights reserved.

1. Introduction

Cyclodextrin glucanotransferase (CGTase, EC 2.4.1.19) is an industrially important enzyme that catalyses the formation of cyclodextrins (CDs) from starch and other related carbohydrates [1] through transglycosylation reactions. CDs can form inclusion complexes with many organic and inorganic compounds within the cavity of their ring structure composed of D-glucose units [2]. Because of this feature, they are widely used in the food, pharmaceutical, cosmetic and chemical industries [3]. Generally, enzymes in industries are formulated in liquid or solid form. Transformation of an enzyme from liquid to solid form improves enzyme stability and shelf life [4]. Due to removal of water from the enzyme, it restricts the enzyme mobility [5] and limits a variety of physical

effects (unfolding, surface adsorption, aggregation) and chemical degradation pathways (covalent bond modification through oxidation and deamidation) during processing, storage and shipping, as discussed elsewhere [6,7].

The most common methods that have been applied to produce enzymes in solid form are freeze drying and spray drying. However, loss of biological activity occurs due to exposure of the enzymes to various types of stresses during these transformation or solidification process. Slow freezing might cause irreversible crystal formation, and excessive heat during spray drying may degrade the compounds [4,8]. In addition, both solidification processes are unable to produce a monodisperse or uniform particle size distribution [9] which is desirable to improve enzymatic performance [10]. With a uniform particle size, particle density and diffusion rates within a matrix can be controlled more precisely, while a size reduction down to the nano-meter scale offers a larger surface area, and hence increased reaction rates [8,11]. In this regard, we decided to explore the feasibility of electrospraying, a well-established liquid atomization method that is capable of producing

* Corresponding author. Tel.: +60 389466359; fax: +60 389464440.

E-mail addresses: nazli@eng.upm.edu.my, ringopie.habibi@gmail.com (M.N. Naim).

monodispersed particles in the sub-micron to nano size range by means of electrostatic forces [12]. We therefore used this method to transform the CGTase enzyme from solution to dry particles.

Electrospraying is a technique that has been widely used in biotechnology applications. The emerging utilization of the electrospraying method is attributed to the unique advantages offered, i.e. the production of monodisperse particles in cone-jet mode, a reduction in the number of molecular aggregates due to the coalescences of droplets with the same polarity, a reduction in the risk of product contamination, operation under ambient conditions, cost effectiveness and simple operation [13,14]. In view of these advantages, a few types of biologically active substances such as DNA, insulin, proteins and enzymes have been successfully electrosprayed with preserved biological activity [11,15,16]. However, only limited reports can be found in the literature on the use of electrospraying to produce enzyme particles, and most of this research has focused on producing particles for pharmaceutical applications [17]. In this study, the production of CGTase particles using the electrospraying method was demonstrated by varying the distance between the needle tip and the collector. Transglycosylation reaction of the electrosprayed enzyme on starch was conducted to study the effect of electrospraying on the enzyme activity as this is a major concern for future application of this route in biocatalysis.

2. Materials and methods

2.1. Materials

CGTase (EC 2.4.1.19) from *Bacillus macerans* was purchased from Amano Enzyme, Inc. (Japan), and was used without further purification. Soluble starch, which was used as the substrate for the CGTase activity assay, was purchased from Merck (Germany). α -CD was purchased from Sigma-Aldrich (M) Sdn. Bhd. (USA). All other chemicals used were of reagent grade.

2.2. Preparation and characterization of CGTase solution

1% CGTase in deionized water was prepared and the zeta potential and particle size of the solution was analysed using a Zetasizer Nano ZS instrument (Malvern Instrument Ltd., Worcestershire) as a function of pH through the auto-titration method. The initial pH of the solution was 6.51 and the value was adjusted from pH 2.0 to pH

10.0 with the addition of 0.1 M HCl and 0.1 M NaOH, respectively. The zeta potential and particle size were measured three times with at least 10 scans for each measurement. The zeta sizer instrument has a built-in Dispersion Technology Software (DTS V4.20) to collect and interpret the data from the device. The electrical conductivity of the solutions was measured using a conductivity probe (Mettler Toledo, Tokyo). All measurements were conducted at room temperature.

2.3. Production of CGTase particles

Atomization of the CGTase solution was performed using an electrospraying system (Fig. 1). The prepared enzyme solution in acetate buffer (100 mM, pH 6) was placed in a 2.5 ml plastic syringe, connected to a 21G flat-end stainless-steel needle which acted as the nozzle. The length, inner diameter and outer diameter of the nozzle were 38.1 mm, 0.51 mm and 0.81 mm, respectively. The flow rate of the solution through the nozzle was controlled by an infusion syringe pump (NE-300, New Era Pump Systems Inc., New York). An electric field was applied to the nozzle using a high voltage power supply (AMI-10K3P, Max-Electronics Co. Ltd., Tokyo) with positive polarity.

A ring electrode with an inner diameter of 18 mm and an outer diameter of 25 mm was positioned perpendicular to the needle tip. The purpose of the ring electrode configuration was to reduce the potential differences between the cone and the grounded collector (counter electrode) [13]. Electrospraying was performed in Taylor-cone jet mode in a closed-type chamber. The distance of the needle tip from the substrate was varied in the range of 10 to 25 cm. The electrospraying modes were observed using a digital camera equipped with a macro lens. Grounded aluminium foil (20 mm \times 25 mm) was used to collect the particles. The deposits on the collector were quantified by weighing using a microbalance (Mettler-Toledo, Tokyo) before and after electrospraying process. The electrospraying current was recorded with a digital electrometer (R8240, Advantest Co. Ltd., Tokyo), which was connected to the grounded collector. The collector which holds the deposited particles was placed in a petri dish and kept overnight in a vacuum desiccators. The samples were then stored at 4 °C for further reactions. The electrospraying parameters used in this study are summarized in Table 1. These parameters were determined after a series of preliminary experiments to establish the cone-jet mode.

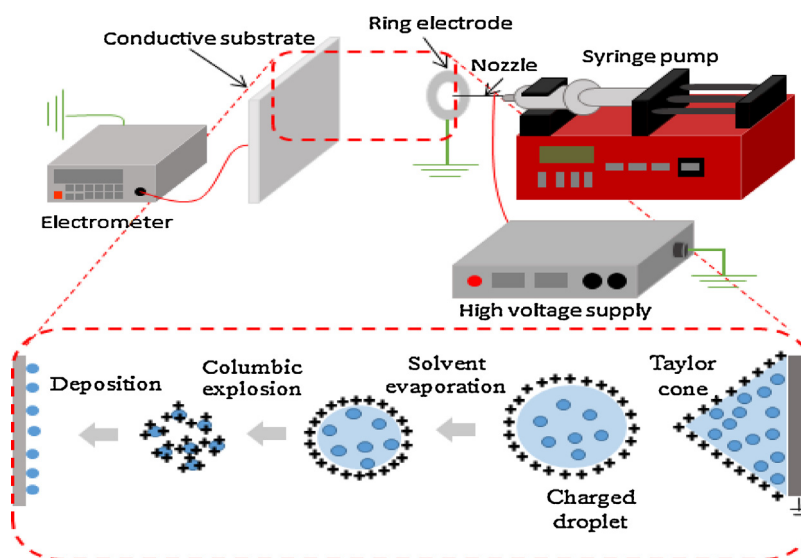


Fig. 1. Electrospraying setup and mechanism.

Table 1

Electrospraying parameters used to obtain a stable cone-jet **Table 2**: Predicted droplet size calculated using scaling law models and comparison of the corresponding particle size calculated using Eq. (4) with SEM.

Parameters	Range
Voltage (kV)	3.44–3.60
Flow rate (ml/h)	0.1–1
Tip to collector distance (cm)	10–25
Electrospraying duration (min)	30

2.4. Scaling laws for estimation of droplet size

Scaling laws proposed by Hartman [18], Fernandez de La Mora [19] and Ganan-Calvo [20] in Eqs. (1)–(3), respectively, were used to estimate size of the electrosprayed droplet:

$$d_d = \left(\frac{\rho \varepsilon_0 Q^3}{\gamma K} \right)^{1/6} \quad (1)$$

$$d_d = 1.66 \varepsilon_r^{-1/6} \left(\frac{Q \varepsilon_r \varepsilon_0}{K} \right)^{1/3} \quad (2)$$

$$d_d = 1.2164 \left(\frac{Q \varepsilon_r \varepsilon_0}{K} \right)^{1/3} \quad (3)$$

where d_d , ρ , ε_0 , Q , γ , K and ε_r represent the droplet diameter, liquid density ($\rho = 1000 \text{ kg/m}^3$), electrical permittivity of the vacuum ($8.8 \times 10^{-12} \text{ C}^2/\text{N/m}^2$), liquid flow rate (m^3/s), surface tension of the liquid ($\gamma = 0.072 \text{ N/m}$), conductivity of the liquid (Sm^{-1}) and relative permittivity (dimensionless number with magnitude of 78.36), respectively [14,21].

Based on the scaling laws, two main parameters that control the droplet size are flow rate and electrical conductivity of the solution [14]. Therefore, to estimate the droplet size, the liquid flow rate was determined experimentally based on the stable cone-jet formation and the solution conductivity was measured using conductivity meter. Then, the rest of the properties were assumed to be equivalent to water which will be used in the calculation as only 1% of CGTase was dispersed in the solution [21].

Assuming that, during the electrospraying process, droplet evaporation occurs without substantial mass loss by other mechanism, then the particle diameter, d_p can be calculated according to Eq. (4) described by [22]:

$$d_d = d_d \phi^{1/3} \quad (4)$$

where ϕ is the volume fraction of the enzyme in the solution.

2.5. Scanning electron microscopy (SEM)

A scanning electron microscope (SEM) (JSM 6510, JEOL, Tokyo) was used to observe the morphology of the collected particles on the aluminium foil. The analysis was performed using an accelerating voltage of 10 kV. Prior to the analysis, all samples were sputter-coated with gold (JFC1200, JEOL, Tokyo) under a vacuum to avoid a charging effect during SEM observations. The sizes of at least 250 particles were determined using ImageJ software (NIH, Bethesda) and the values are presented as the average.

2.6. Fourier transform infra-red (FTIR) spectroscopy

FTIR spectroscopy was used to study the changes in CGTase functional groups (primary and secondary amino groups) after electrospraying. The analysis was conducted using a Nicolet Nexus-470 spectrometer (Thermo Electron Corp., Waltham). Samples prepared by normal drying were used as the control and the spectra were collected in the range of 4000 to 800 cm^{-1} with 32 scans and a scan resolution of 4 cm^{-1} .

2.7. Enzyme activity

Enzyme activity analysis was carried out to investigate the effect of the electrospraying process on the catalytic activity of the enzyme. The dry mass of the deposits were calculated based on the changes in mass of the collector before and after electrospraying. CGTase activity was measured as α -CD formation activity, as previously described [23] with slight modifications [24]. The α -CD concentration was assayed by the decrease in absorbance at 506 nm caused by the formation of a methyl orange α -CD complex. For this analysis, the electrosprayed enzyme was dissolved in 1 ml of reaction mixture containing 1% soluble starch solution in 50 mM phosphate buffer (pH 6) by placing the collector containing the deposited particles into the solution [25]. Then, the collector was removed before the reaction mixture was heated to 60°C for 5 min. The reaction was stopped with immediate cooling in chilled water followed by the addition of 0.1 ml of HCl (1.2 M). After that, 2 ml of methyl orange (final concentration of 0.035 mM) were added into the reaction solution. The mixtures were maintained at room temperature for 15 min. Absorbance was measured using a UV-vis spectrometer (Ultrospec 3100 Pro, GE Healthcare Sdn Bhd., Kuala Lumpur). One unit of enzyme activity was defined as the amount of enzyme that produced $1 \mu\text{M}$ of α -CD per minute under the assay conditions.

2.8. Statistical analysis

Statistical analyses were performed using GraphPad Prism version 6.0 (La Jolla, CA) software. A statistical difference between groups was analyzed using the Mann-Whitney non-parametric test (for comparison of two groups) and the one-way analysis of variance (ANOVA) (for comparison of more than two groups). p -Values < 0.05 were considered significant.

3. Results and discussion

3.1. Characterization of CGTase in liquid phase

To investigate the behavior of CGTase in the liquid phase, the zeta potential and particle size were plotted as a function of pH (Fig. 2). The isoelectric point of the solution was found to be at pH 3.82. At this point, the zeta potential value, which correlates with the net surface charge of the enzyme, is zero. Thus, charge repulsion among the enzyme is minimal, which increases the tendency of particle aggregation and results in larger particles. This mechanism is referred to as the specific electrostatic interaction effect [6]. However, the largest particle size here was obtained at a pH lower than the isoelectric point (pH 3.23), where the net charge was positive (+5.75 mV). Therefore, in this case, the effect of non-specific electrostatic interactions is more dominant than

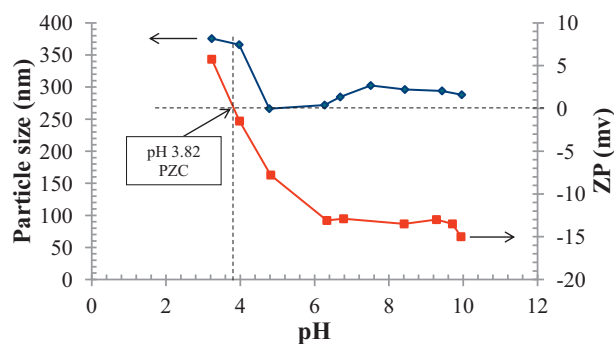


Fig. 2. Particle size and zeta potential of CGTase solution as a function pH.

the specific electrostatic interaction [26]. Non-specific electrostatic interactions involve destabilization of the folded enzyme conformation at a pH level below or above isoelectric point due to the higher charge density of the folded enzyme than its unfolded counterpart. As a consequence, the electrostatic free energy is reduced, which leads to enzyme aggregation [6].

The smallest particle size was observed in the range pH of 4.78 to 6.27 due to an increase in the enzyme net charge, which increased the repulsive forces among particles and enhanced solution stability. Above pH 6.27, even though the zeta potential value was at the highest magnitude, the particle size increased gradually as a result of non-specific electrostatic interactions, as discussed previously. Based on this result, the stable region for the enzyme is in the pH range of 4.78 to 6.27. Therefore, the electrospraying enzyme solution was prepared at pH 6, considering both solution stability and optimum pH for maintaining the enzyme activity as provided by the enzyme manufacturer.

Prior to electrospraying, a 1% enzyme in acetate buffer solution (100 mM, pH 6) was freshly prepared. This concentration was chosen after screening the electrospraying of CGTase without dilution. It was found that the cone-jet mode could not be formed, and the SEM analysis revealed that the enzyme existed in large agglomerates (data not shown). This phenomena could be occurred due to the high probability of particle collisions at very high enzyme concentrations [27], thus increasing the tendency to agglomerate. Additionally, a low concentration guarantees minimal non-specific associations during electrospraying [28]. Other studies have proposed that the conductivity of the prepared solution prior to electrospraying should be in the range of 1 $\mu\text{S}/\text{cm}$ to 10 mS/cm [16]. The electrical conductivity of the non-diluted enzyme was found to be 35.6 mS/cm . Dilution of the enzyme to 1% lowered the conductivity value to 8.36 mS/cm , which is within the suggested range.

3.2. Electrospraying with cone-jet mode

There are a few modes that can be used when conducting an electrospraying experiment. These modes can be classified as dripping, pulsing, cone-jet and multi-jet [29]. The ability of electrospraying to be operated under cone-jet mode is the key advantage that differentiates this method with other particle production methods. The cone-jet mode offers the generation of monodispersed particles with a narrow size distribution. Additionally, the size of particles can be controlled, depending on solution properties and processing parameters, to benefit the desired application.

The electrospraying mechanism under cone-jet mode is illustrated in Fig. 1. It involves four major processes: generation of charged droplets, shrinkage of the droplets due to solvent evaporation, repeated disintegration of the droplets into dry particles and, finally, collection or deposition of the particles [30]. To generate a charged droplet, a strong electric field is required, typically on the order of 10^6 V/m. The applied field at the capillary tip is given by [21]:

$$E_c = \frac{2V_c}{(r_c \ln 4d/r_c)} \quad (5)$$

where V_c , d and r_c are the applied voltage, distance between the capillary and counter-electrode and radius of the capillary, respectively. The required electric field at the capillary (onset electric field, E_{on}) for the formation of a jet at the apex of the cone is determined by the following equation [31]:

$$E_{on} \approx \left[\frac{(2\gamma \cos \theta)}{(\varepsilon_0 r_c)} \right]^{0.5} \quad (6)$$

where γ is the surface tension of the solvent, θ is the half angle of the cone which was determined photographically by Taylor as 49.3° [21] and ε_0 is the permittivity of the vacuum. Combining Eqs. (5) and (6), the onset voltage, V_{on} can be predicted as:

$$V_{on} \approx \left[\frac{(r_c \gamma \cos \theta)}{(2\varepsilon_0)} \right] \ln \left(\frac{4d}{r_c} \right) \quad (7)$$

Substituting $\varepsilon_0 = 8.8 \times 10^{-12} \text{ J}^{-1} \text{ C}^2$ and $\theta = 49.3^\circ$, Eq. (7) can be simplified as:

$$V_{on} \approx 2 \times 10^5 (\gamma r_c)^{0.5} \ln \left(\frac{4d}{r_c} \right) \quad (8)$$

Based on these equations, the predicted E_{on} and V_{on} for our experiment were calculated to be 6.04×10^6 V/m and 3.30 kV, respectively, while the electric field at the capillary tip, E_c , was 7.12×10^6 V/m (with an applied voltage of 3.50 kV). It should be noted that the applied voltage should be a few hundred volts higher than V_{on} to establish stable electrospraying operation. Therefore, the applied voltage of 3.44 to 3.60 kV that was observed for stable cone-jet mode in our study is in accordance with the theoretical calculation.

3.3. SEM analysis

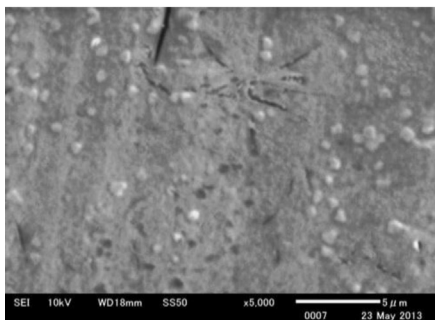
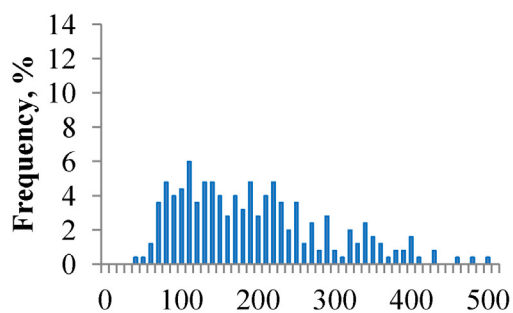
Micrographs obtained from the SEM analysis of the deposited CGTase particles on aluminium foil with various collection distances are shown in Fig. 3. From this figure, we can see the morphological changes of the particles as the collection distance was varied from 10 to 25 cm. "Wet" deposition was observed when the enzyme particles were collected at a distance of 10 cm. The existence of solvent residue with the enzyme particles showed that incomplete solvent evaporation had occurred. Wet deposition usually produces inhomogeneous semi-solid, flat particles which solidify after deposition [32]. Single enzyme particles with enzyme clusters containing a few particles were observed in Fig. 4. The number of clusters was reduced as the collection distance increased. At the longest collection distance (25 cm), no enzyme clusters (aggregation) existed and only the single/individual particle morphology was observed. The size distributions of the deposited particles were plotted to study the changes in particle size with collection distance. It was found that the longest collection distance produced the smallest particles with a narrow size distribution, which confirmed that droplet shrinkage and fission occurred before deposition on the grounded collector.

The deposition mechanisms at variable distances are illustrated in Fig. 4. With an increase in collector distance, the droplets have a longer flight time and solvent evaporation time, giving more time for columbic explosion to occur, hence leading to the production of smaller particles [10,33]. Columbic explosion or fission occurs once the charged droplet reaches a Rayleigh limit, where the charge repulsion on the surface of the droplet is greater than the surface tension which holds the droplets together [34]. A loss in droplet mass during a single fission event is typically not large enough to affect particle size. However, as the droplet undergoes multiple fissions, the resulting particle size will be reduced [22]. Based on this result, it was confirmed that by changing the tip to collector distance, the electrospraying method employed in this study was capable of producing nearly monodisperse CGTase nanoparticles with an average size of 75 ± 34 nm.

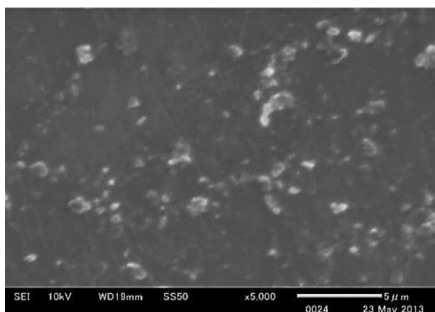
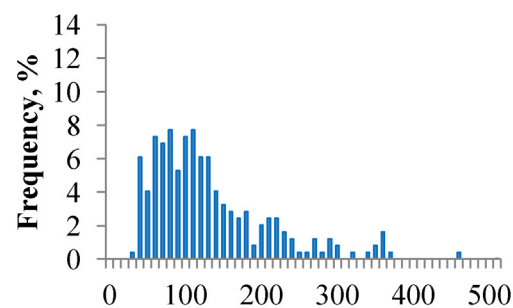
3.4. Predicted droplet size from scaling laws

The particle sizes obtained from the SEM images (Fig. 4) were compared with the estimated droplet size from scaling laws modeled by Hartman et al. [18], de la Mora and Loscertales [19] and

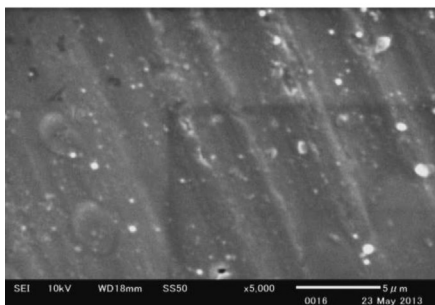
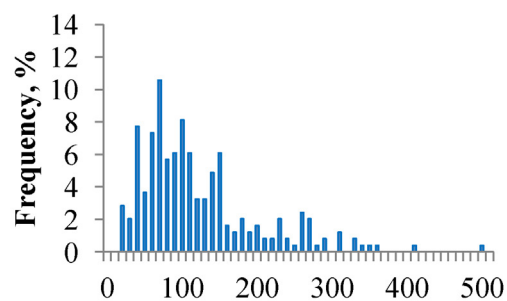
A) 10 cm

Mean: 201 ± 117 nm

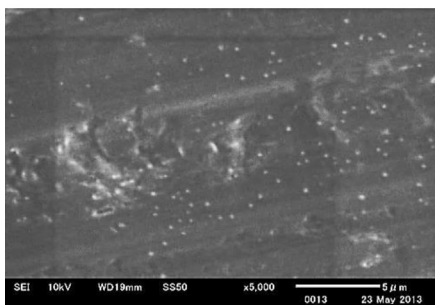
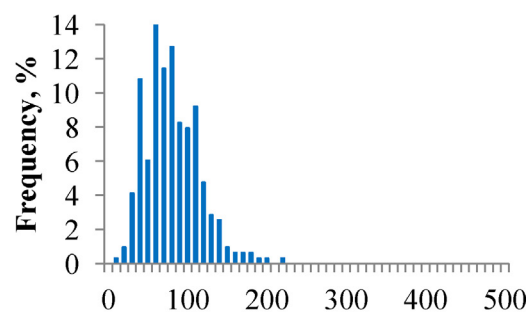
B) 15 cm

Mean: 128 ± 80 nm

C) 20 cm

Mean: 117 ± 79 nm

D) 25 cm

Mean: 75 ± 34 nm

Particle size, nm

Fig. 3. SEM images of deposited CGTase particles on aluminium foil and its size distribution with varied distance.

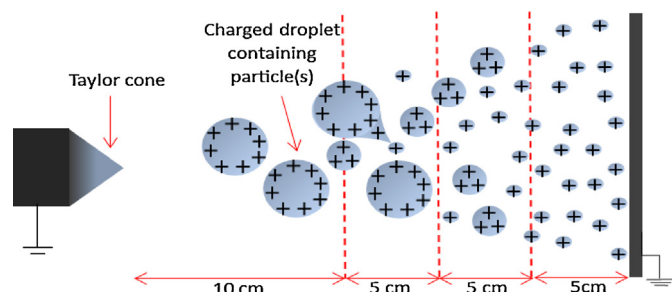


Fig. 4. Mechanism of droplet deposition with varied distance.

Table 2

Predicted droplet size calculated using scaling law models and comparison of the corresponding particle size calculated using Eq. (4) with SEM.

Model	Droplet size (nm)	Particle size (nm)
[19]	229	49
[20]	516	111
[18]	382	82
SEM	–	75 ± 34*

* Average particle size of CGTase deposited at 25 cm from the needle tip (smallest solid particles as indicated in SEM images).

Ganan-Calvo [20] in Eqs. (1)–(3), respectively, to validate the effectiveness of the developed electro spraying system. The parameters to predict the mean droplet size were obtained from the literature as stated in Section 2.4. In Table 2, it is shown that the particle sizes obtained from SEM were in agreement with the predicted sizes.

The particle sizes calculated from the Hartman model were the closest to the experimental results. Therefore, the predicted droplet size from the Hartman model was further used to determine the fissility of the droplet, X , using Eq. (9), which represents the possibility of the droplet to undergo fission. The equation was described by [35] as the ratio of the electrostatic repulsion force and the force acting on the droplet surface:

$$X = \frac{q^2}{64\pi^2 \gamma \epsilon_0 (d_d/2)^3} \quad (9)$$

where q is the droplet charge which can be determined from the following equation:

$$q = \frac{d_d I}{V} \quad (10)$$

The current, I was measured with an electrometer connected to the collector while the droplet velocity, V , at variable collector distances, D , can be expressed as [15]:

$$V = 1.9 \left(\frac{Q}{\eta D} \right) (\gamma \epsilon_0 d_d)^{1/2} \quad (11)$$

where η is viscosity of the solution which equivalent to water viscosity ($1.8 \times 10^{-5} \text{ N s m}^{-2}$).

Salata [35] has demonstrated that for $X < 1$, the chances of droplets disintegration are minimal. Droplet fission occurs at $X \geq 1$ where the charge repulsion on the droplet surface increases after successive solvent evaporation. As a result, the droplet

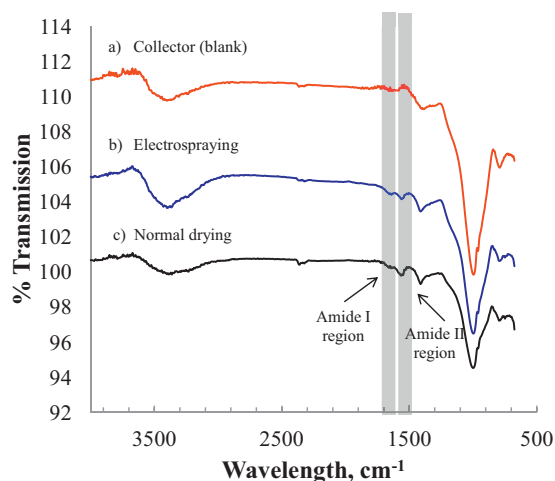


Fig. 5. FTIR spectra of CGTase deposited on a glass slide by electro spraying and the normal drying approach.

become unstable and disintegrates into several progeny droplets. In the case of $X \gg 1$, the droplet is break down into very fine progeny droplets “whose fineness however has a limit”. The X value at different collector distance obtained in this study is presented in Table 3. It was found that all $X \gg 1$ which indicates that the mother droplets has undergone subsequent fission event before reaching the collector. Longer collector distance allows the mother droplets to experience more fission event than shorter distance, thus producing smaller particles as observed in Fig. 4.

3.5. Fourier transform infra-red (FTIR) spectroscopy

Fig. 5 shows the IR spectra of CGTase particles produced through the electro spraying method and normal drying method from the same CGTase solution. For this analysis, the enzyme was deposited on a glass substrate instead of aluminium foil. This is because, from our preliminary measurements, the peaks from the enzyme and the aluminium foil cannot be distinguished due to the existence of a few overlapping peaks. CGTase characteristic peaks are the bands related to primary and secondary amino groups [36]. The primary amide I band, which usually absorbs at $\sim 1650 \text{ cm}^{-1}$, is caused by C=O stretching vibrations which are sensitive to the secondary structure of the enzyme backbone. Therefore, it was used for secondary structure analysis. The amide II band is mainly due to C–N stretching and N–H bending vibrations in the enzyme backbone near 1550 cm^{-1} [37]. The bands at 1644 cm^{-1} and 1560 cm^{-1} , which correspond to amide I and amide II, respectively, can be seen in the electro spraying CGTase spectra (Fig. 5(c)). This spectrum was compared with the CGTase spectra obtained using the normal drying method, where the bands were observed at 1642 cm^{-1} and 1564 cm^{-1} for amide I and II. It was shown that the spectrum of the electro sprayed enzyme was nearly identical to that of the dehydrated enzyme.

Table 3

Current, velocity, charge and fissility of droplets at varied collector distances.

Collector distance (cm)	Current (nA)	Droplet velocity (m/s)	Droplet charge (C)	Fissility (X)
10	40	1.82	8.38×10^{-15}	2.51
15	35	1.22	7.34×10^{-15}	1.92
20	31	0.91	6.50×10^{-15}	1.51
25	28	0.73	5.87×10^{-15}	1.22

3.6. Effect of electro spraying on enzyme activity

In an enzymatic reaction, the performance of the enzyme is usually determined by its catalytic activity, which often affected by many factors. Electro spraying is a safe and gentle process for biomolecules, and causes no damage to the native structure [12]. However, several conditions in the electro spraying process may contribute to enzyme activity losses [15]. Therefore, proper selection of electro spraying conditions is needed to preserve the activity.

Electrochemical reactions inside the capillary during electro spraying may cause a dramatic drop in the pH of the solution, as previously reported [38]. In our case, we intended to minimize this effect with the use of a buffered solution in which the pH is stable. Intensification of the electric field around the particles during solvent evaporation could interfere with protein conformation, which may also cause denaturation [11]. Regarding this problem, the counter electrode's ring configuration that was used in this study is beneficial to prevent a rapid increase in the electric field near the cone-tip due to the uniform external electric field generated by the ring electrode [39].

Other factor, such as the formation of a corona discharge, may occur during the electro spraying process. Corona discharge generates hot atoms and radicals that might react with protein molecules. An empirical equation to predict the onset of electric field corona initiation, E_{CO} , for a capillary with a radius $r > 100 \mu\text{m}$ has been derived as [39]:

$$E_{CO} = 3 \times 10^6 \left(\frac{1 + 0.03}{r^{0.5}} \right) \quad (12)$$

By using this equation, the onset corona, E_{CO} , was found to be $8.63 \times 10^6 \text{ V/m}$, which shows that an additional $1.51 \times 10^6 \text{ V/m}$ electric field (with regards to the electric field applied at the capillary, E_c) would be required to initiate corona formation. Meanwhile, current measurement is very important to ensure the stability of the electro spraying system. Complete enzyme inactivation at a high electro spraying current ($>500 \text{ nA}$) and voltage ($>7 \text{ kV}$) has been reported by [15]. Gomez et al. [11] suggested that electro spraying should be conducted at spraying current lower than 100 nA to avoid droplet charging. The use of a low conductivity solution as well as a low electro spraying current ($28\text{--}40 \text{ nA}$) in our system aimed to minimize this effect. Under these mild conditions and with the precautions discussed above, the factors that could potentially damage the enzyme were minimized during electro spraying, but complete preservation of enzyme activity is not guaranteed.

In order to study the effect of enzyme activity after the droplet solidification, each of the electro spraying experiment condition was conducted in Taylor cone-jet mode. During the process, the electro spraying conditions were varies (flow rate, distance, and deposition time) and all the enzyme activities were recorded and analysed. For reference purpose, one the electro sprayed sample was compared with the native enzyme (same weight percentage). The deposited CGTase was placed in a desiccator overnight prior to the enzyme activity analysis. A surface consisting of drops of the native enzyme solution was also prepared and treated in the same way for reference purposes. The enzyme activity was characterized by observing the decrease in absorbance caused by the formation of methyl orange α -CD complexes. For the reference comparison (Fig. 6), the result shows that the difference between the native and electro sprayed enzyme activity is not statistically significant ($p > 0.05$) which indicates that the electro spraying system used in this study has no adverse effect on the enzyme.

In term of the enzyme activity, the size of the solidified droplets has more significant effect in comparison with the weight percentage of the solidified droplets. To study the condition, the tip to collector distance was investigated by varying the distance from 10 to 25 cm. Based on the graph shown in Fig. 7, increased in

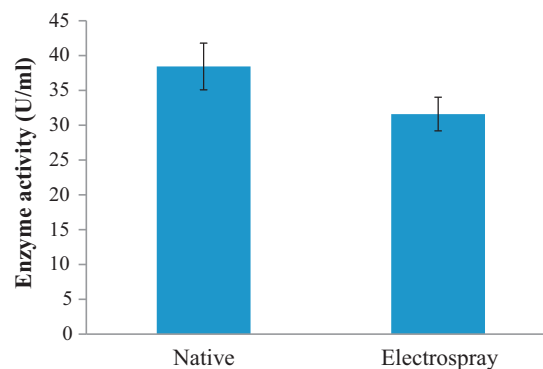


Fig. 6. Activity of electro sprayed enzyme and the native enzyme.

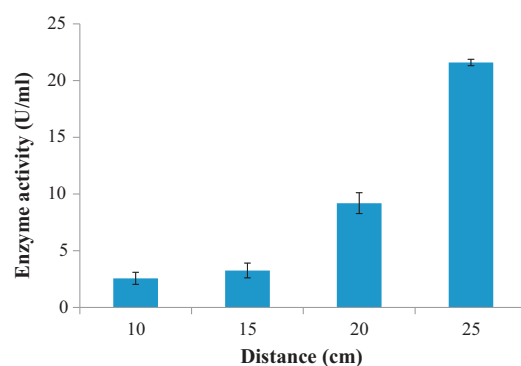


Fig. 7. Effect of collector distance on enzyme activity.

collector distance resulted in significant increase of enzyme activity ($p < 0.0001$). This result can be explained by the results obtained from SEM analysis in Fig. 3, where the longest tip to collector distance produced the smallest particle size. The increase in enzyme activity with smaller particle size is related to the increased dissolution rate and saturation stability of the particles with a large surface area [40] in accordance with the Noyes Whitney and Ostwald–Freundlich equations [41]. Additionally, the wet deposition observed at the nearest collection distance may have broken the enzyme intra molecular disulphide bonds and formed new intermolecular bonds, which could have led to enzyme aggregation, resulting in low enzyme activity. This phenomenon occur due to the low elastic modulus of the protein deposited in its hydrated state, which is up to 20 times lower than that of the protein in the dry state, which reduces its ability to adapt its native conformation [15,25].

4. Conclusions

- (1) The electrostatic charge applied in electro spraying process and conducted in cone-jet mode produced nanometer-sized CGTase enzyme particles with an average particle size of 75 nm.
- (2) Increasing the distance from tip to collector significantly reduce the particle size due to droplet fission. The droplet fission mechanism was utilized to evaporate the droplets's solvent.
- (3) Dry particles collected at 25 cm (longest) shows the highest enzyme activity than other distances.
- (4) The functional groups of solidified enzyme were preserved and undeteriorated after the electro spraying process.
- (5) Activity of the native and electro sprayed enzyme was not statistically different which indicates that electro spraying is a promising method for producing solidified enzyme particles in nanometer-order

Acknowledgements

We thank to Dr. Motoyuki Iijima, Mr. Pramujo Widiatmoko, Mr. K. Kusdianto and Mr. Keisuke Naito (Tokyo University of Agriculture and Technology) for their guidance and help with the analysis. This research was supported by the Science-fund, Ministry of Science, Technology and Innovation, (MOSTI) Malaysia (Project No: 02-01-04-SF1469), Ministry of Education Malaysia (FRGS/2/2013/TK05/UPM/02/15), JSPS Kakenhi No. 23560904 (IWL) and Research Entity Initiative (REI) grant by Universiti Teknologi MARA (UiTM) (Project no. 600-RMI/DANA/5/3/REI (2/2013)). S. Saallah holds a scholarship from Ministry of Higher Education (MOHE), Malaysia under the SLAB scheme.

References

- [1] Qi Q, Mokhtar MN, Zimmermann W. Effect of ethanol on the synthesis of large-ring cyclodextrins by cyclodextrin glucanotransferases. *J Inclusion Phenom Macrocyclic* 2007;57:95–9.
- [2] Atasanova N, Kitayska T, Yankov D, Safarikova M, Tonkova A. Cyclodextrin glucanotransferase production by cell biocatalysts of alkaliphilic bacilli. *Biochem Eng J* 2009;46(3):278–85.
- [3] Ferrarotti SA, Bolivar JM, Mateo C, Wilson L, Guisan JM, Roberto F-L. Immobilization and stabilization of a cyclodextrin glycosyltransferase by covalent attachment on highly activated glyoxyl-agarose supports. *Biotechnol Prog* 2006;22:1140–5.
- [4] Roy I, Gupta MN. Freeze-drying of proteins: some emerging concerns. *Bio-technol Appl Biochem* 2004;39(2):165–77.
- [5] Maa Y, Sellers SP. Solid-state protein formulation. In: Smales CM, James DC, editors. *Therapeutic Proteins: Methods and Protocols*. Totowa, NJ: Humana Press Inc. 308; 2009. p. 265–85.
- [6] Chi EY, Krishnan S, Randolph TW, Carpenter JF. Physical stability of proteins in aqueous solution: mechanism and driving forces in nonnative protein aggregation. *Pharm Res* 2003;20(9):1325–36.
- [7] Mahler HC, Friess W, Grauschopf U, Kiese S. Protein aggregation: pathways, induction factors and analysis. *J Pharm Sci* 2009;98:2909–34.
- [8] Peltonen L, Valo H, Kolakovic R, Laaksonen T, Hirvonen J. Electro-spraying, spray drying and related techniques for production and formulation of drug nanoparticles. *Expert Opin Drug Deliv* 2010;7(6):705–19.
- [9] Xie J, Wang CH. Encapsulation of proteins in biodegradable polymeric microparticles using electro-spray in the Taylor cone-jet mode. *Biotechnol Bioeng* 2007;97(5):1278–90.
- [10] Gholami A, Tavanai H, Moradi AR. Production of fibroin nanopowder through electro-spraying. *J Nanopart Res* 2010;13(5):2089–98.
- [11] Gomez A, Bingham D, Juan L, Tang K. Production of protein nanoparticles by electro-spray drying. *J Aerosol Sci* 1998;29(5/6):561–74.
- [12] Jaworek A. Electro-spray droplet sources for thin film deposition. *J Mater Sci* 2006;42(1):266–97.
- [13] Yurteri CU, Hartman RPA, Marijnissen JCM. Producing pharmaceutical particles via electro-spraying with an emphasis on nano and nano structured particles—a review. *KONA Powder Part J* 2010;28:91–115.
- [14] Jaworek A. *Electro-spray Technology for Thin-Film Deposition*. Hauppauge, N.Y.: Nova Science Publishers Inc.; 2010. ISBN 9781617612015.
- [15] Morozov VN. Electro-spray deposition of biomolecules. *Adv Biochem Eng Biotechnol* 2010;119:115–62.
- [16] Lee YH, Wu B, Zhuang WQ, Chen DR, Tang YJ. Nanoparticles facilitate gene delivery to microorganisms via an electro-spray process. *J Microbiol Methods* 2011;84(2):228–33.
- [17] Xie J, Marijnissen JCM, Wang CH. Microparticles developed by electrohydrodynamic atomization for the local delivery of anticancer drug to treat C6 glioma in vitro. *Biomaterials* 2011;27:3321–32.
- [18] Hartman RPA, Brunner DJ, Camelot DMA, Marijnissen JCM, Scarlett B. Jet break-up in electrohydrodynamic atomization in the cone-jet mode. *J Aerosol Sci* 2000;31(1):65–95.
- [19] Fernandez de La Mora J, Loscertales IG. The current emitted by highly conducting Taylor cones. *J Fluid Mech* 1994;260:155–84.
- [20] Ganan-Calvo AM. The surface charge in electro-spraying: its nature and its universal scaling laws. *J Aerosol Sci* 1999;30(7):863–72.
- [21] Kebarle P, Verkerk UH. Electro-spray: from ions in solution to ions in the gas phase, what we know now. *Mass Spectrom Rev* 2009;1–20.
- [22] Hogan Jr CJ, YunkM, Chen DR, Lenggoro IW, Biswas P, Okuyama K. Controlled size polymer particle production via electrohydrodynamic atomization. *Colloids Surf, A: Physicochem Eng Aspects* 2007;311(1):67–76.
- [23] Lejeune A, Sakaguchi K, Imanaka T. A spectrophotometric assay for the cyclization of cyclomaltohexaose (α -cyclodextrin) glucanotransferase. *Anal Biochem* 1989;181:6–11.
- [24] Higuti IH, Silva PA, Papp J, Okiyama VME, Andrade EA, Marcondes AA, et al. Colorimetric determination of α and β -cyclodextrins and studies on optimization of CGTase production from *B. firmus* using factorial designs. *Braz Arch Biol Technol* 2004;47:837–41.
- [25] Morozov VN, Morozova TY. Electro-spray deposition as a method to fabricate functional active protein films of proteins and other biopolymers. *Anal Chem* 1999;71:1415–20.
- [26] Majhi PR, Ganta RR, Vanam RP, Seyrek E, Giger K, Dubin PL. Electrostatically driven protein aggregation: β -lactoglobulin at low ionic strength. *Langmuir* 2006;22:9150–9.
- [27] Maximova N, Dahl O. Environmental implications of aggregation phenomena: current understanding. *Curr Opin Colloid Interface Sci* 2006;11:246–66.
- [28] Hilton GR, Benesch JLP. Two decades of studying non-covalent biomolecular assemblies by means of electro-spray ionization mass spectrometry. *J R Soc Interface* 2012;9(70):801–16.
- [29] Lenggoro IW, Okuyama K, Fernandez de la Mora J, Tohge N. Preparation of ZnS nanoparticles by electro-spray pyrolysis. *J Aerosol Sci* 2000;31:121–36.
- [30] Naim MN, Abu Bakar NF, Iijima M, Kamiya H, Lenggoro IW. Electrostatic deposition of aerosol particles generated from an aqueous nanopowder suspension on a chemically treated substrate. *Jpn J Appl Phys* 2010;49(6):06GH17.
- [31] Smyth WF. The use of electro-spray mass spectrometry in the detection and determination of molecules of biological significance. *TRAC, Trends Anal Chem* 1999;18(5):335–46.
- [32] Bock N, Woodruff MA, Hutmacher DW, Dargaville TR. Electro-spraying, a reproducible method for production of polymeric microspheres for biomedical applications. *Polymers* 2011;3(1):131–49.
- [33] Hazeri N, Tavanai H, Moradi AR. Production and properties of electro-sprayed sericin nanopowder. *Sci Technol Adv Mater* 2012;13(3):035010.
- [34] Seto T, Maekawa S, Osone S, Kawamura K, Yamauchi T, Otani Y. Formation of highly charged nanodroplets by condensation–electro-spray device. *Chem Eng Sci* 2013;85:46–9.
- [35] Salata OV. Tools of nanotechnology: electro-spray. *Curr Nanosci* 2005;1:25–33.
- [36] Amud AE, da Silva GRP, Tardioli PW, Soares CMF, Moraes FF, Zanin GM. Methods and supports for immobilization and stabilization of cyclomalto-dextrin glucanotransferase from *Thermoanaerobacter*. *Appl Biochem Biotechnol* 2008;146(1–3):189–201.
- [37] Mei Y, Miller L, Gao W, Gross RA. Imaging the distribution and secondary structure of immobilized enzymes using infrared microspectroscopy. *Biomacromolecules* 2003;4:70–4.
- [38] Van Berkel CJ, Feimeng Zhou JTA. Changes in bulk solution pH caused by the inherent controlled-current electrolytic process of an electro-spray ion source. *Int J Mass Spectrom Ion Processes* 1997;162:55–67.
- [39] Park H, Kim K, Kim S. Effects of a guard plate on the characteristics of an electro-spray in the cone-jet mode. *J Aerosol Sci* 2004;35(11):1295–312.
- [40] Williams III RO, Overhoff KA. Advances in drug delivery technologies for nanoparticulates. In: Peppas NA, Zach Hilt J, Brock Thomas J, editors. *Nanotechnology in Therapeutics*. United Kingdom: Horizon Bioscience; 2007. p. 65–89.
- [41] Sun J, Wang F, Sui Y, She Z, Zhai W, Wang C, Deng Y. Effect of particle size on solubility, dissolution rate, and oral bioavailability: evaluation using coenzyme Q₁₀ as naked nanocrystals. *Int J Nanomed* 2012;7:5733–44.